DRIFT4SKIM 2018

SKIM Proof-of-concept validation campaign

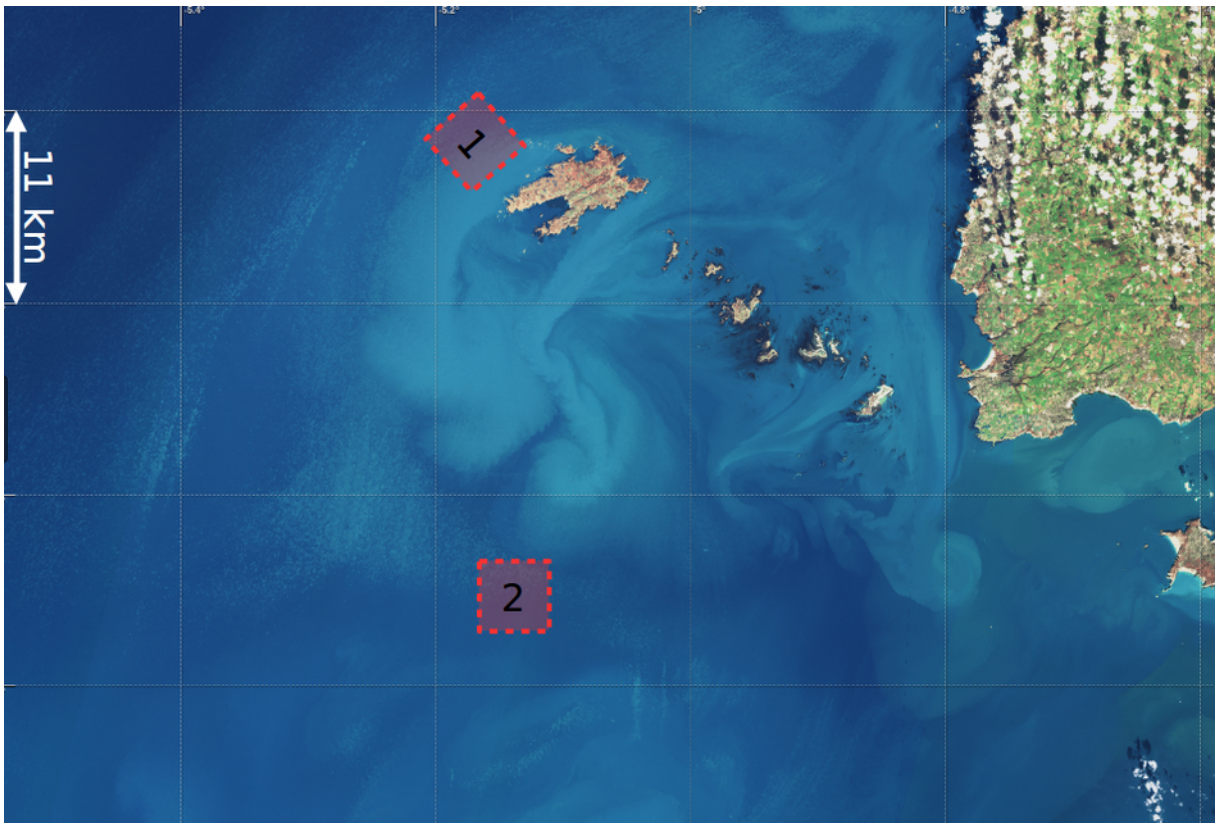

Deliverable 3 - Final Report

ESA Contract No. 4000126110/18/NL/FF/gp
IFREMER Contract No. 18/2216801/F

L. Marié, B. Chapron, F. Nouguier, P. Sutherland, IFREMER, France
F. Ardhuin, CNRS, France
F. Collard, L. Gaultier, ODL, France,
F. Boy, J.-C. Lalaurie, CNES, France

v1.0, November 15, 2019

Document change record

Author	Modification	Issue	Rev	Date
L. Marié	Initial release	1.0	1.0	11/2019

Applicable Documents

Reference	Title
[AD-1]	SKIM Mission Requirements Document (ESA-EOPSM-SKIM-MRD-3218)
[AD-2]	DRIFT4SKIM2018 Technical Support for the SKIM 2018 Drifters Campaign (ESA Contract N° 4000126110/18/NL/FF/gp)

Reference Documents

Reference	Title
[RD-1]	DRIFT4SKIM 2018 Campaign Implementation Plan (ESA ref. 4000126110/18/NL/FF/gp/D1)
[RD-2]	SKIM Campaign Data Acquisition Report (CNES ref. DSO/SI/TR-2019.01210)
[RD-3]	Marié, L., F. Collard, F. Nouguier, L. Pineau-Guillou, D. Hauser, F. Boy, S. Méric, C. Peureux, G. Monnier, B. Chapron, A. Martin, P. Dubois, C. Donlon, T. Casal, F. Ardhuin: "Measuring ocean surface velocities with the KuROS and KaRADOC airborne near-nadir Doppler radars: a multi-scale analysis in preparation of the SKIM mission", *subm. to* Ocean Science, doi: 10.5194/os-2019-77, 2019.
[RD-4]	Caudal, G., Hauser, D., Valentin, R., and Gac, C. L.: KuROS: A New Airborne Ku-Band Doppler Radar for Observation of Surfaces, J. Atmos. Ocean Technol., 31, 2023–2245, doi:10.1175/JTECH-D-14-00013.1, 2014.
[RD-5]	Drift4SKIM2018 In-situ/airborne optical data hard disk and Data Acquisition Report (ESA ref. 4000126110/18/NL/FF/gp/D2)
[RD-6]	Earth Explorer 9 Candidate Mission SKIM – Report for Mission Selection(ESA ref. ESA-EOPSM-SKIM-RP-3550)
[RD-7]	Nouguier, F.: Remote Sensing Spatial Simulator (R3S), Tech. Rep. SKIM-MPRC-TN6-V1.0-LOPS-2019, ESA, 2019.

ESA STUDY CONTRACT REPORT

ESA Contract No: **4000126110/18/NL/FF/gp**	SUBJECT: **DRIFT4SKIM2018 SKIM proof-of-concept validation campaign**	CONTRACTOR: **IFREMER**
ESA CR No:	No. of Volumes: **1** This is Volume No: **1**	CONTRACTOR'S REFERENCE: **18/2216801/F/D3**

ABSTRACT:

As part of the Detailed design and feasibility studies of the Sea Surface Kinematics Multiscale (SKIM) 9th Earth Explorer program candidate mission, ESA initiated the Drift4SKIM field campaign, with the aim to evaluate the feasibility of measuring the in-situ Total Surface Current Velocity (TSCV) using pulse-pair Doppler radars.

The campaign took place from November 20th to November 27th, 2018, in the Iroise Sea, west of the french Atlantic coast, chosen for its wave climate and its strong tidal regime, and featured both airborne and in-situ data collection components.

Airborne data collection consisted in Ku- and Ka-band pulse-pair Doppler measurements performed using the KuROS and KaRADOC radars from an ATR-42 aircraft, and optical (visible and TIR) observations of the sea surface performed from a PA-23 aircraft. Both aircrafts were operated by the french research aircrafts facilities, SAFIRE.

In-situ operations consisted in the deployment of two moored buoys providing observations of wind, waves and surface current shear, and the deployment of a large number (~130) of drifting buoys measuring currents at different depths (0.4, 1, 2, 5 and 15 m). The deployments were performed from french R/V Thalia, operated by the french research fleet operator GENAVIR, and rigid inflatable boats Bermudes and Lipouille, operated by a local subcontractant.

Names of authors:

L. Marié, B. Chapron, F.Nouguier, P. Sutherland (IFREMER / LOPS)

F. Ardhuin, (CNRS / LOPS)

F. Collard, L. Gaultier (ODL)

F. Boy, J.-C. Lalaurie (CNES)

NAME OF ESA STUDY MANAGER: **Tânia Casal**	** ESA BUDGET HEADING:

Contents

1 Introduction....5
1.1 Context....5
1.2 Campaign implementation....5
2 Campaign results....6
2.1 Airborne observations....7
2.1.1 Radar observations....7
2.1.2 Optical observations....10
2.2 In-situ observations....11
2.2.1 Observations from R/V Thalia....11
2.2.1 Currents observations....13
2.2.2 Sea state observations....16
3 Conclusions and perspectives....18
Acknowledgements....20

1 Introduction

1.1 Context

Surface currents are poorly known over most of the oceans. The aim of the Sea surface Kinematics Multiscale (SKIM) mission proposal, which was selected for detailed design and feasibility studies in the European Space Agency 9th Earth Explorer program, is to implement a satellite-borne Doppler Waves and Current Scatterometer to fill this observation gap.

SKIM is based on a combination of two instruments, a SRAL-type nadir altimeter, and a Ka-band near-nadir pencil-beam conically scanning Doppler scatterometer. This last instrument is a new concept and benefits from very little heritage from previous missions.

With this in mind, ESA funded the Drift4SKIM field campaign, with the aim [RD-1]

to demonstrate that pulse-pair Doppler radar observations of the ocean surface can be used to retrieve a meaningful ocean surface current.

1.2 Campaign implementation

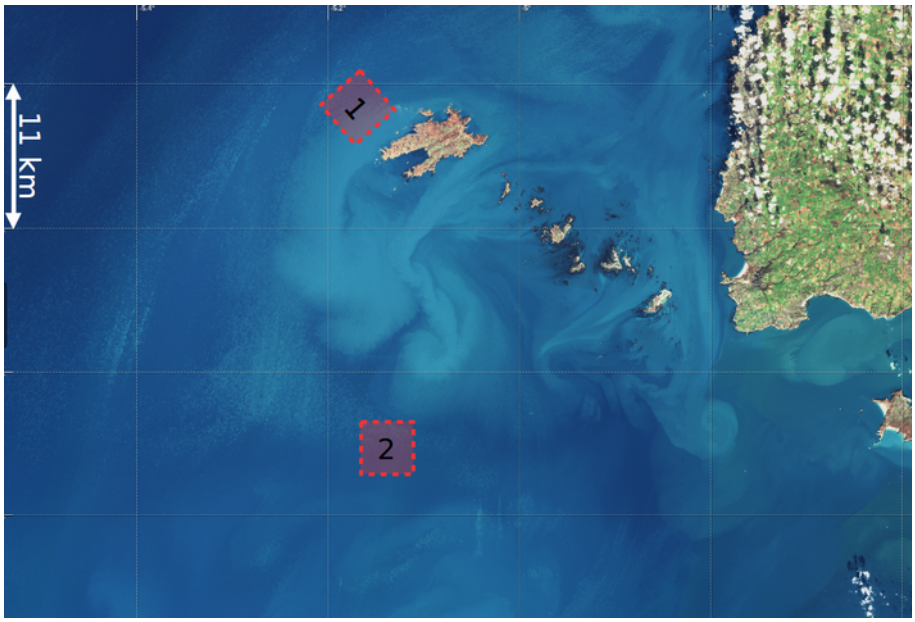

Figure 1: Sentinel-2 MSI false-color image of the campaign location, taken on 2017-02-14. The two areas marked with red rectangles are refered to in the text as the Keller Race and Offshore areas (respectively marked 1 and 2).

A comprehensive description of the data collection effort has been given in [RD-5].

The campaign took place from November 19th to November 28th, 2018 in the Iroise Sea (Figure 1), off the French Atlantic coast, with sea states representative of the open ocean, and a well known tide-dominated current regime. It was composed of a large airborne radar observation effort, complemented by an extensive in-situ field campaign.

The airborne component involved two aircrafts (the ATR-42 and PA-23 of the french scientific aircraft fleet, operated by SAFIRE) and implemented:

- Ku-band radar observations of the sea surface performed using the fan-beam, conically scanning, range resolved pulse-pair KuROS radar, originally developped in the framework of the CFOSAT mission Cal/Val program [RD-4]
- Ka-band radar observations of the sea surface performed using the pencil-beam, footprint-limited pulse-coherent KaRADOC radar, based on the SWALIS instrument originally developped in the framework of the SWOT mission Cal/Val program.
- Optical observations of the sea surface performed using a suite of cameras covering an extensive range of wavelengths and observation geometries (wide-angle TIR/VNIR/RGB, fisheye panchromatic).

The in-situ campaign involved the 25 m R/V “Thalia”, from the Flotte Oceanographique Française, and the two Rigid Inflatable Boats (RIBs) “Bermudes” and “Lipouille” which performed:

- Deployment and recovery of a moored buoy equipped with an IMU and an Acoustic Doppler Current Profiler (“TREFLE” buoy). This buoy provided sea state as well as current measurements until 2018/11/22, when it capsized. After this point, only the sea state measurements could be used.
- Deployment of a moored buoy equipped with an acoustic anemometer/gas analyzer instrument for eddy-correlation flux measurements (“FLAME” buoy). The IMU used to correct the data of these instruments for platform motion failed, precluding their analysis.
- Deployment of a large number of drifting buoys of different types and drogue depths, providing a consistent view of lagrangian currents from 40 cm to 15 m below the surface.
- Deployment of 10 drifting buoys providing directional sea state measurements.

Finally, the campaign benefited from the additional observations collected by a wave-rider buoy and an HF-radar surface current monitoring system operated respectively by CEREMA and Shom, both french governmental agencies.

2 Campaign results

Overall, the Drift4SKIM campaign was highly successful, and the collected data will serve for many years as a reference dataset for near-nadir phase-coherent microwave ocean backscatter studies. Considerable effort has already been devoted to the analysis of the data, in the framework of the SKIM Report for Mission Selection preparation [RD-6]. Due to the very tight timeframe, the analysis was however very far from exhaustive, and focussed on a comparison of drifter-based TSCV estimates with Ka-band pulse-pair doppler radar observations. The comparison was found satisfactory, provided account was properly taken of the wave Doppler bias, which was estimated from sea-state measurements. This work is summarized in an article submitted in June 2019 to Ocean Science Discussions [RD-3].

2.1 Airborne observations

2.1.1 Radar observations

2.1.1.1 KuROS observations:

A large effort was devoted to the analysis of the KuROS Ku-band radar data. This work provided very valuable insight in the imaging process (reported in the appendices of [RD-3]), and allowed to thoroughly validate the R3S simulator (see Figure 2).

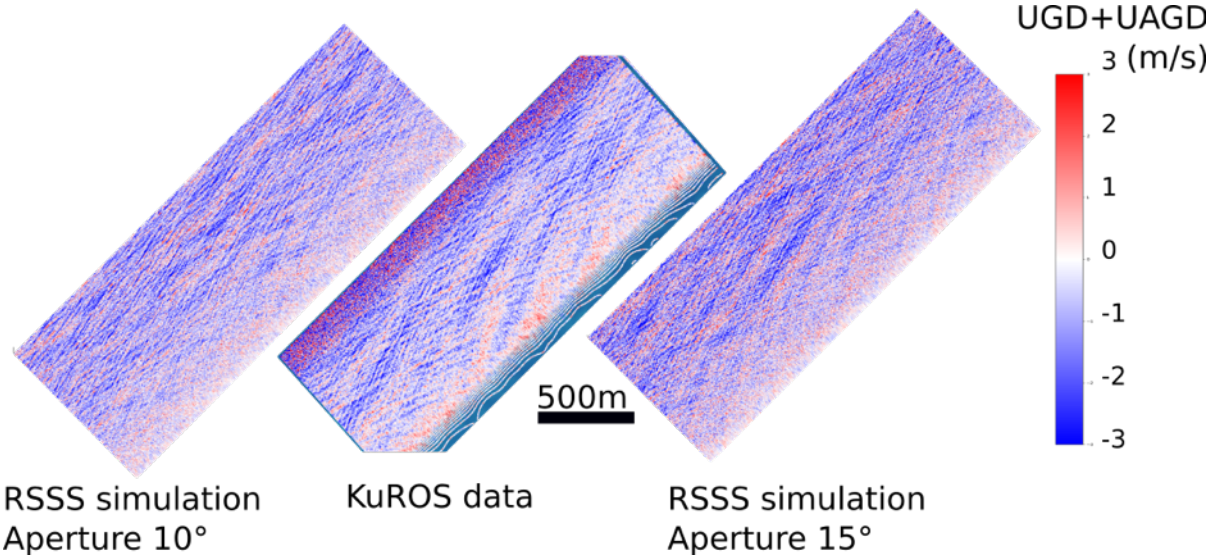

Figure 2: center: platform-motion corrected KuROS Doppler data segment, taken on 2018/11/22 with a port-looking antenna. Left and right: R3S simulated Doppler data for 10° (left) and 15° (right) azimuthal apertures (note that the simulations are based on random sea surfaces generated using the in-situ measured statistics). Taken from [RD-3].

However, the conclusion of this work was that the quite broad antenna radiation diagram of KuROS was not well suited to the measurement of TSCV:

- for up- or down-track observations, the uncertainty in incidence angle translated to a contamination by the platform motion of the order of 2 m/s, which was much too large with respect to the SKIM mission requirements. Reducing the incidence angle uncertainty would require achieving nadir radar-to-ground range estimations with an accuracy better than 10 cm, which is clearly out of reach of the KuROS system.
- for cross-track observations, naturally occuring cross-section modulations due to long waves are strong enough to overcome the radiation pattern drop in azimuth. In this situation, the radar Doppler signal is strongly affected by contributions coming from the front or the back of the trajectory, which the platform motion corrections can not compensate in the absence of information regarding the backscattering elements azimuth. This can be seen in Figure 2, for instance: the large values of motion-corrected Doppler seen in the observations, and reproduced in the simulation results, are not orbital velocities, but rather the range-motion with respect to the platform of highly reflective wave flanks located either in the forwards or aftwards parts of the instantaneous swath. As the instrument only provides access to the pulse-pair signal, SAR techniques could not be implemented to mitigate this effect.

2.1.1.2 KaRADOC observations:

Ka-band KaRADOC observations, in contrast, turned out much easier to analyse. This was rather unexpected as the Drift4SKIM experiment was the first deployment of the instrument, which had not even been extensively tested in the lab for lack of time. Allowance made for a number of minor mishaps, resulting for instance in unreliable calibration of backscattering level, or for a severe degradation of noise level for incidences different from 12°, the operation of the instrument can be considered to have been very successful.

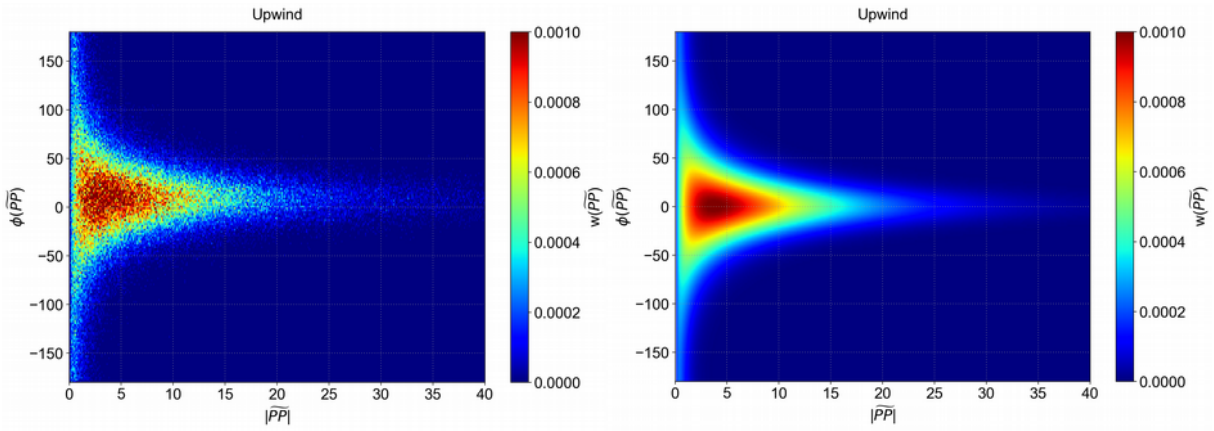

Figure 3: Left: joint histogram of the modulus (x-axis) and phase (y-axis) of the instantaneous pulse-pair signal, observed during an upwind-viewing leg on 2018/11/22. Right: corresponding theoretical distribution, using shape parameter values estimated from the data.

As shown for instance in Figure 3, the observed signal statistics could be found to conform very closely to theoretical expectations. In particular, the signal from this campaign thus provides a very useful dataset to test theories of speckle noise influence on the pulse-pair phase signal statistics in the cross-track viewing geometry.

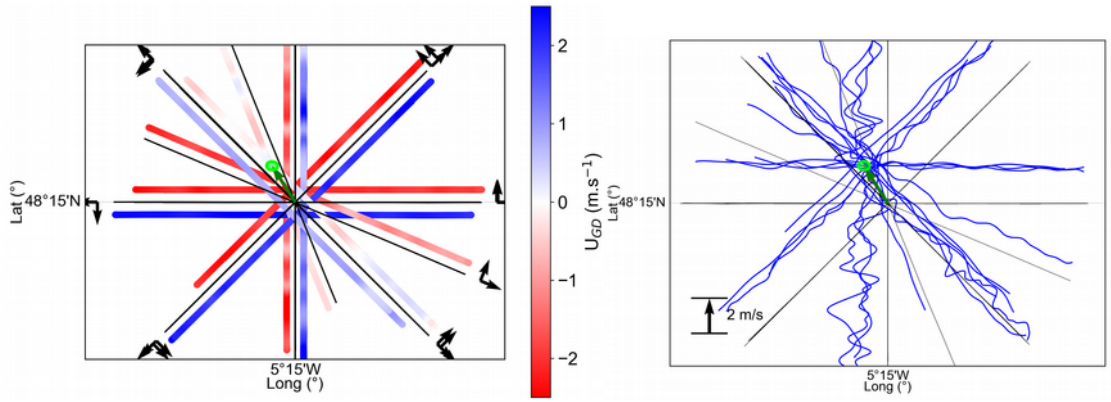

Figure 4: Left: instantaneous values of low-pass-filtered U_{GD} for the star pattern flight performed over the Offshore area on 2018/11/22. The arrows show the flight direction and look direction. Right: same data, represented as a shift from the flight track proportional to U_{GD}. Data collected along the different tracks are consistent with a single-valued vector. The green arrow and ellipse show the best least-squares vector fit to the data and the estimated 1-σ error ellipse (Figure taken from [RD-3]).

Due to the very narrow radiation diagram of the antenna, the Doppler signal could be much

better corrected for platform motion, and provided much more stable values of U_{GD}. Figure 4 (left) shows the instantaneous values of U_{GD}, filtered to remove the fast variations due to waves, along to the flight tracks of 2018/11/22. Clearly, the data obtained along tracks directed in opposite directions have opposite signs, indicating they indeed represent the projection of a vector along opposite directions. The mean values also depend in a plausible way with observation direction. Figure 4 (right) then shows the same data, with instantaneous U_{GD} represented as a shift from the flight track. In this representation, lines corresponding to data collected in both directions along each track overlap, showing the agreement is indeed quantitative, and the intersections of the bundles of lines corresponding to the data collected along the different tracks accumulate in roughly the same locus, showing the data indeed behave like different projections of a unique vector, (within of course slight variations due either to non-stationarity of the sea state and/or current, or to as yet unaccounted for phenomena).

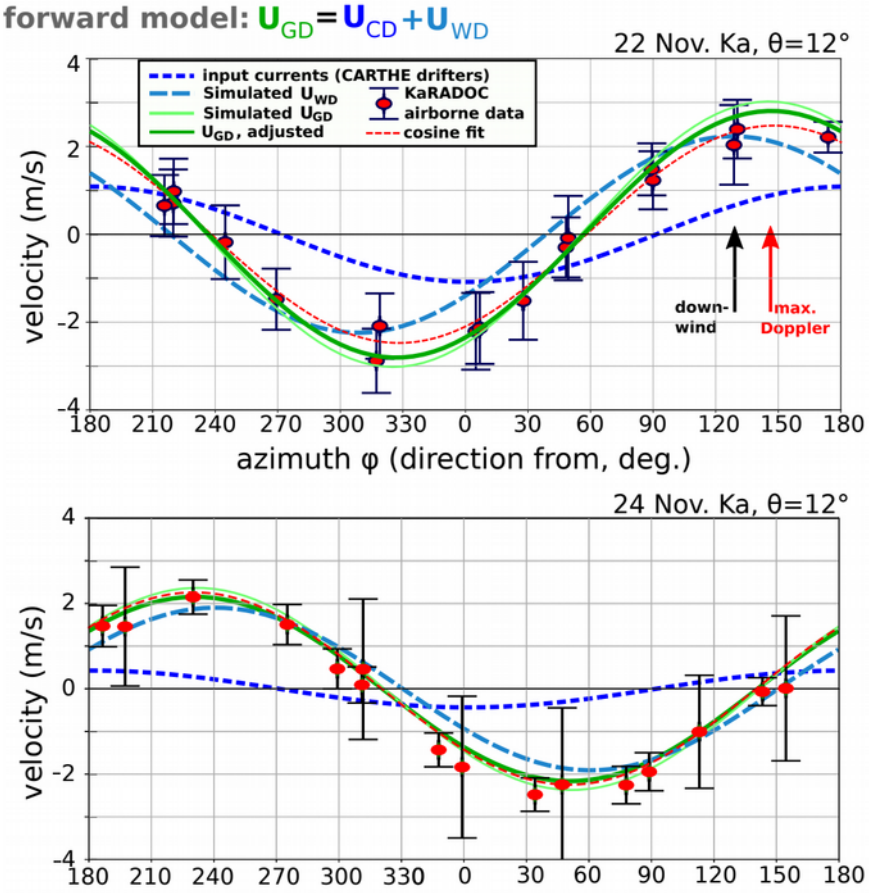

Figure 5: Comparison of KaRADOC and in-situ measurements of TSCV for 2018/11/22 (top) and 2018/11/24 (bottom). The KaRADOC mean U_{GD} values along the different tracks are plotted as red dots. The CARTHE drifters U_{CD} is plotted in dashed dark blue. Adding to the CARTHE drifters U_{CD} the wave Doppler computed using the directional sea state statistics evaluated from the TREFLE data results in the light green curve. Further applying a 10% reduction in the wave Doppler results in the dark green curve (Figure taken from [RD-3]).

Figure 5, also taken from [RD-3], further represents the observed Ka-band U_{GD} as a function of observation azimuth, together with the CARTHE drifters U_{CD} and the wave doppler U_{WD} estimated using the TREFLE directional sea state data. The observations fall very neatly on a sinusoidal curve, once again showing they are compatible with projections along different

look directions of a single vector. The other interesting element of this graph is the very close agreement between the radar Doppler data and the projection along the radar line-of-sight of the sum of the CARTHE drifters estimate of TSCV and of the estimated U_{WD}. This agreement can be further improved by reducing U_{WD} by 10%. We have at present no justification for this reduction, but this agreement shows that obtaining a meaningful estimate of the TSCV from Ka-band Doppler measurements is clearly feasible, provided a directional sea state spectrum is jointly available.

2.1.2 Optical observations

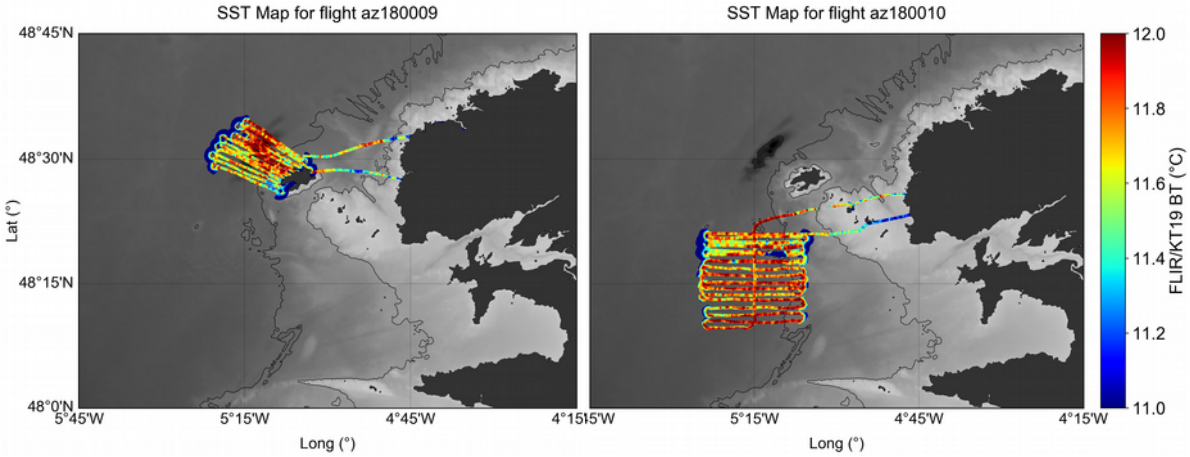

Figure 6: Brightness temperature maps produced using LagadIR on 2018/11/21 over the Keller Race (left) and Offshore (right) areas. Cold areas during turns are caused by the decrease of IR sea surface emissivity at high incidence angles. Kilometer-scale variations of brightness temperature are probably due to changes in atmospheric absorption.

For lack of time, the analysis of these data has not been pursued past the Quality Check stage. Brightness Temperatures mosaics have been generated from the infrared observations (see for instance Figure 6), which clearly indicate that no large-scale temperature gradient was present over the area during the campaign, excluding the possibility of density-gradient induced currents and vertical shear.

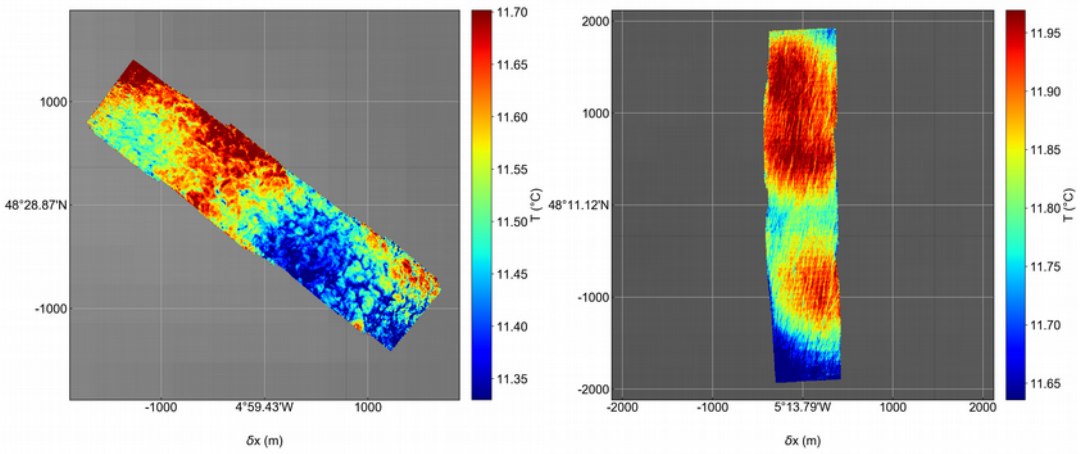

Figure 7: Details of brightness temperature maps obtained produced using LagadIR data acquired on 2018/11/20 at 14:04:35 UTC (left, to the north-west of Ushant) and 14:18:38 UTC (right, in the south of the Offshore zone). x- and y-axis scales are in meters from the mid-point. Kilometer-scale variations of

temperature are probably due to changes in atmospheric water content.

These mosaics however evidence an interesting diversity of small-scale SST patterns, some examples of which are shown in Figure 7, which will clearly deserve further study, notably in combination with the other cameras (RGB, panchromatic fish-eye).

2.2 In-situ observations

2.2.1 Observations from R/V Thalia

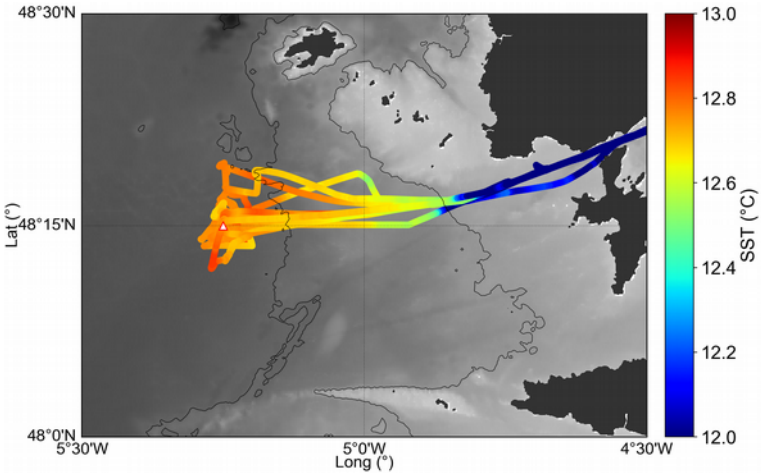

Figure 8: Trajectory of R/V Thalia for all campaign days. The track colour represents the Sea Surface Temperature from the ship thermosalinograph intake SBE38 thermometer, located at 3 m depth.

Figure 8 represents the R/V Thalia track and sea surface temperature for the whole duration of the campaign. A SST front is clearly visible at 4°45'W. This front separates the continentally-influenced waters of the "Rade de Brest" from those of the open Iroise/Celtic Seas. This front lies clearly far inshore of the areas were the campaign operations took place. These data also show that SST is as expected weakly variable, spatially as well as temporally, in the Offshore area.

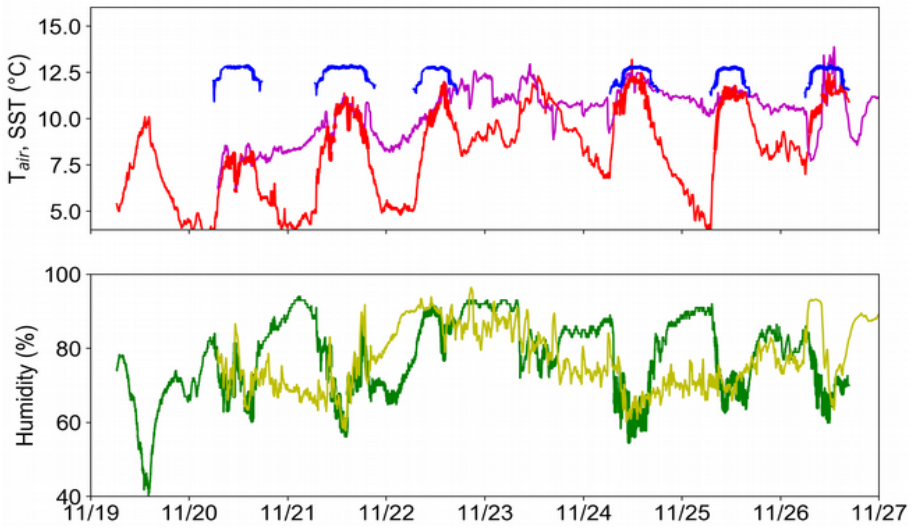

Figure 9: R/V Thalia meteorological data for whole the campaign period. Top: Air temperature from BATOS package (red), from FLAME buoy (magenta), SST from TSG intake SBE38 (blue). Bottom: Air humidity from BATOS package (dark green), from FLAME buoy (light green). The SST data are only available when

the ship is at sea. The FLAME buoy was deployed on 9:45 UTC on 11/20, broke its tether on 5:30 UTC on 11/23, and was recovered by Ushant fishermen at 5:45 UTC on 11/26.

Figure 9 represents the data from the R/V Thalia meteorological sensors. The SST data are only available when the ship is actually sailing, i.e. during the daytime of 11/20, 11/21, 11/22, 11/24, 11/25, 11/26. On each day, the SST data display a large step when the ship crosses the front at the Rade de Brest entrance. The air temperature measured by the ship BATOS package displays a marked diurnal cycle, but comparison with the FLAME buoy data shows that a large part of the cycle amplitude is due to spurious or geographic effects (the air temperature is affected by land mass effects when the ship is in port), and that the cycle was much weaker offshore. The FLAME air temperature remained lower than the daytime SST over the Offshore zone during the period when the buoy was tethered, as well as during the period when it drifted towards Ushant. During the whole experiment, the ocean surface boundary layer was thus convectively unstable, pointing to convection as a forcing factor for the structures apparent in the airborne brightness temperature maps of Figure 7.

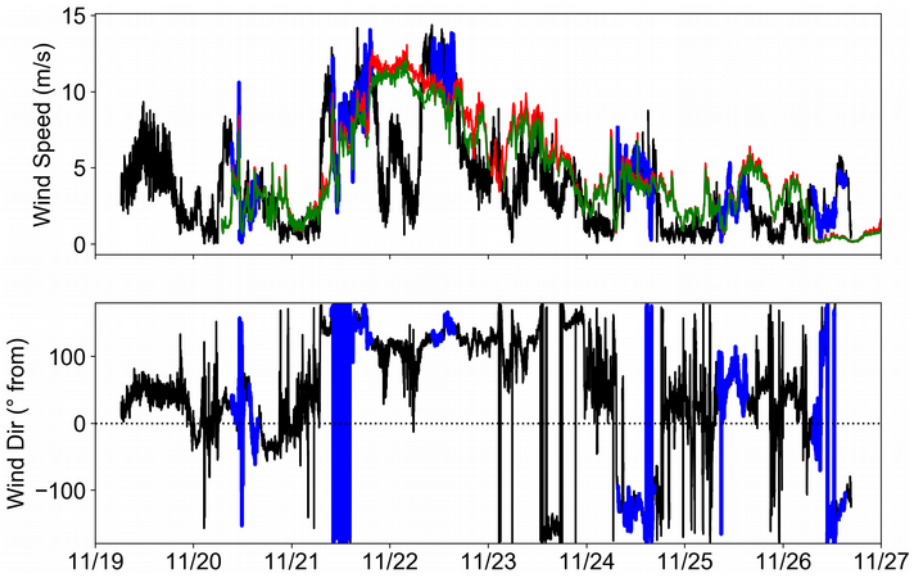

Figure 10: R/V Thalia meteorological data for whole the campaign period. Top: 10 m height wind speed from Thalia BATOS package (black), during periods when the ship is at sea and facing within 60° from wind (blue), 2 m wind speed from FLAME Gill Metpak package (red), 2 m wind speed from FLAME IRGASON package (green). Bottom: 10 m wind direction from Thalia BATOS package (black), during periods when the ship is at sea and facing within 60° from wind (blue).

Figure 10 shows the available wind data for the duration of the experiment. Wind speed was inferior to 5 m/s until the morning of 11/21, then rose rapidly to its peak value of 12 m/s in the early morning of 11/22, then decreased progressively until the morning of 11/24, after which it remained below 5 m/s. Due to the failure of the FLAME buoy IMU, only the Thalia BATOS anemometer was able to report wind direction. As apparent in Figure 10, winds were mostly northerly on 11/20, then veered to south-easterly during the strong wind episode, and in particular during the 11/22, which was analysed in depth in [RD-3]. The direction was then variable during subsequent days, winds being south-westerly on 11/24, north-easterly on 11/25, and variable, but very weak, on 11/26.

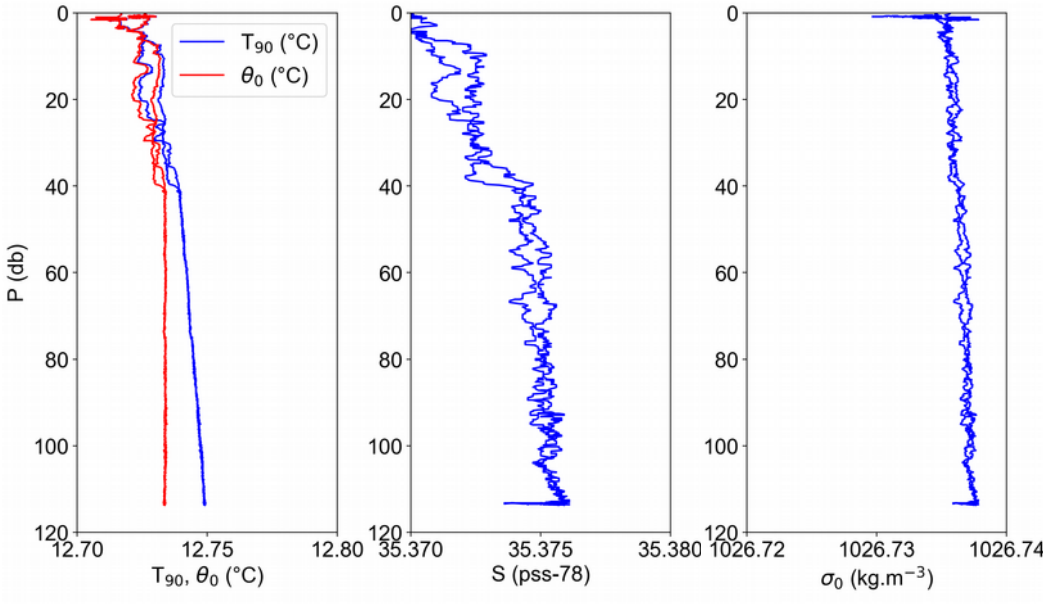

Figure 11: Data from CTD profile performed on 2018/11/21, 10:35 UTC at the TREFLE/FLAME deployment point at 48°15'N, 5°15'W.

Figure 11 finally shows the data from a CTD cast performed on 2018/11/21, 10:35 UTC at the TREFLE/FLAME deployment point. As expected in the Offshore area in this season, the stratification is very weak, corresponding to a surface-to-bottom potential density difference smaller than 0.003 g/L. This stratification is of mixt origin, being the result of a very weak unstable thermal stratification (the difference between in-situ and potential temperature at 110 m is actually significant with respect to the surface gradients) and a very weak stable haline stratification. Both components of stratification are surface-intensified. Temperature differences between the down-cast and up-cast profiles, though of the order of 0.01°C, have a magnitude similar to the total surface-to-bottom range. Such minute temperature gradients, though they are measurable and could be used to diagnose convection in the surface layer, are far too weak to bear any influence on the flow dynamics.

2.2.1 Currents observations

2.2.1.1 TREFLE ADV/ADCP observations

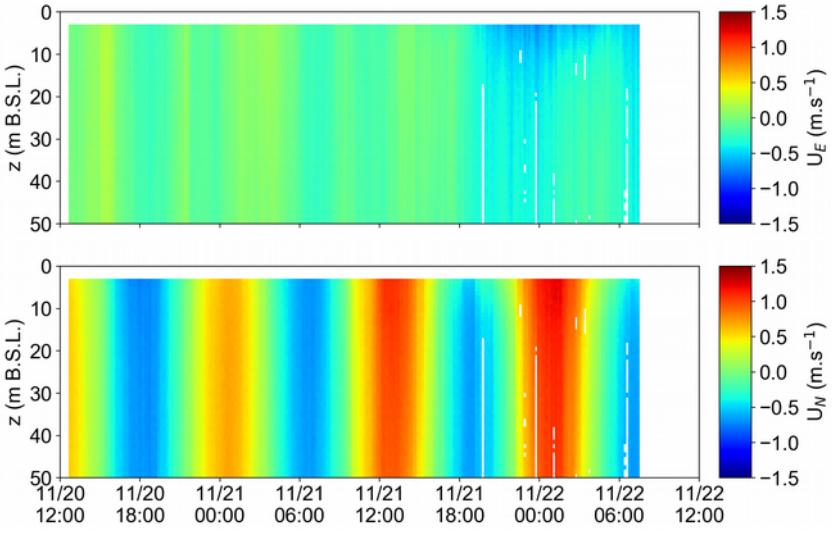

Figure 12: Current profiles (up: eastward component, bottom: northward

component) measured from 3 m to 50 m below sea surface by the downward-looking ADCP mounted on the TREFLE buoy, moored at 48°15'N, 5°15'W, before it capsized on 2018/11/22, 7:30 UTC.

Figure 12 presents the current profiles measured by the downward-looking ADCP mounted on the TREFLE buoy before it capsized. These data show as expected a very strong barotropic tidal signal. The current oscillates mainly in the N/S direction with maximal values of the order of 1 m/s, increasing slightly with time between 11/20 and 11/22 under the effect of the fortnightly cycle, and minimal values of the order of 0.1 m/s. Though its polarization is essentially linear, the current veers slightly clockwise over each tidal period. A slight shear is visible in the vicinity of the surface towards the end of the period, as the wind attains its maximal strength.

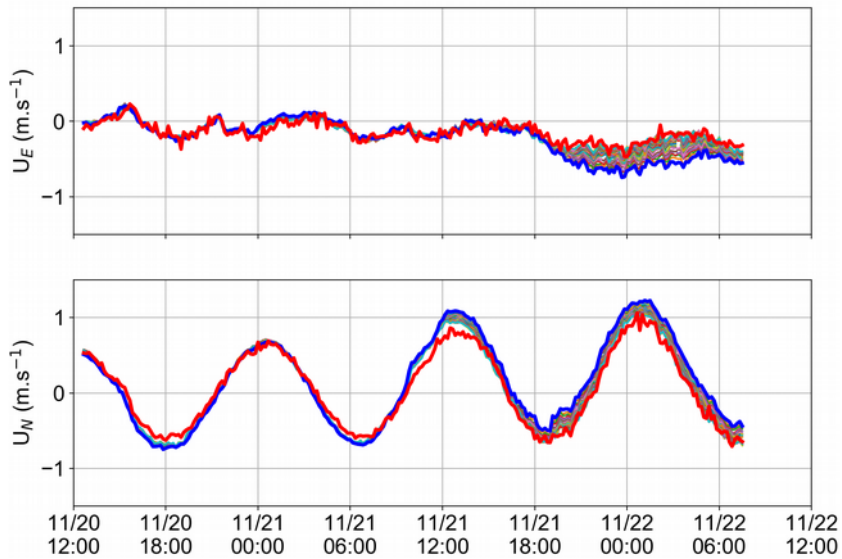

Figure 13: Nortek Vector Acoustic velocimeter data (red) compared to the ADCP timeseries (other colors, 1 measurement bin every 1 m starting at 3 m below surface. The thick blue curve represents the first valid data bin of the ADCP) over the TREFLE useful measurements period.

One must however be careful in the interpretation of this surface shear: Figure 13 shows the timeseries of ADCP data for the depth range 3 m to 50 m below surface, together with the data of the Nortek Vector acoustic velocimeter that was also fitted to the buoy, the measurement volume of which was located 30 cm below the sea surface. Surprisingly, the velocimeter data are not consistent with the surface layer shear measured by the ADCP, but rather with the bulk currents measured deeper in the water column. In fact, interpreting current measurements from a surface-following buoy has to be done very carefully to disentangle properly Stokes drift shear and Eulerian shear. Such a careful analysis could not be performed on the Drift4SKIM data set for lack of time.

2.2.1.2 Drifters observations

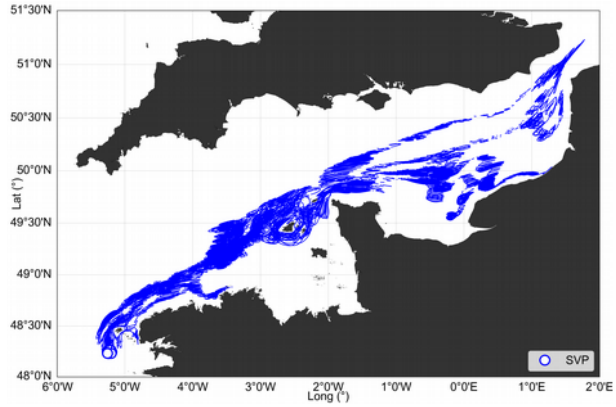

Figure 14: Full tracks of the SVP drifters (15 m depth holey-sock drogues) deployed during the experiment.

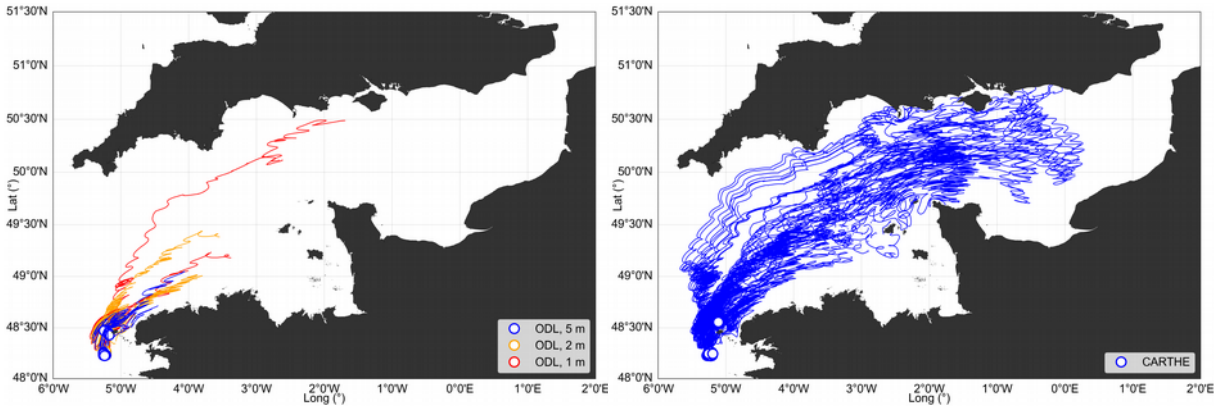

Figure 15: left: Full tracks of the ODL drifters (5, 2, 1 m depth Microstar™ drogues) deployed during the experiment. Right: Full tracks of the CARTHE™ drifters deployed during the experiment.

Figure 14 and Figure 15 present the complete (*i.e.* not restricted to the experiment duration) tracks of the drifters deployed during the experiment. Though the data are interesting in their own right (the SVP drifters by themselves represent a significant addition to the drifter trajectory database in the English Channel), the comparison between the two extremes of the depth range instrumented during the experiment, 15 m depth (Figure 14) and 0.4 m (Figure 15 right) makes very plain the difference in drifting behaviour between the two water depths. During calm weather periods, the CARTHE trajectories do bear some degree of similarity with the SVP trajectories. In high-wind periods, however, the CARTHE buoys tend to drift much faster and cover large distances, while the SVP trajectories seem essentially unaffected. Correctly estimating and predicting this difference is a key issue for the exploitation and validation of SKIM data.

2.2.2 Sea state observations

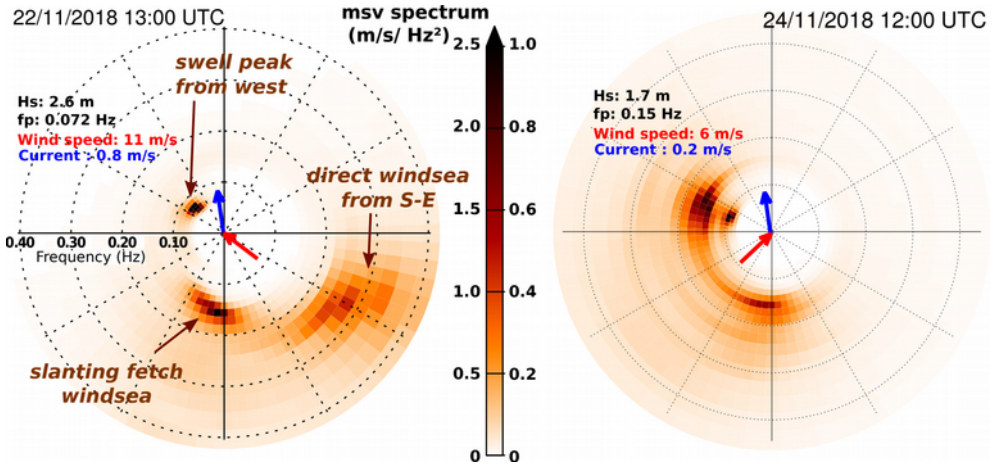

Figure 16: Directional sea state spectra obtained using the "Maximum Entropy Method" from the TREFLE buoy on 2018/11/22 (left) and from Spoondrift buoy SPOON10 on 2018/11/24 (right), together with HF radar currents (blue) and ECMWF wind (red). Shading indicates energy spectral density in the direction ***from*** *which waves arrive (Figure taken from [RD-3]).*

Figure 16 shows typical examples of directional wave spectra observed during the campaign, produced using the so-called "Maximum Entropy Method" using data collected by the TREFLE buoy (left) and buoy SPOON10 (right). Swell coming from the west-north-west was present during the whole period with varying intensity, associated with a much more variable wind sea, which followed wind changes. Interestingly, a clear effect of the fetch obstruction due to the island of Sein, to the south of the area, could be observed during southerly wind periods.

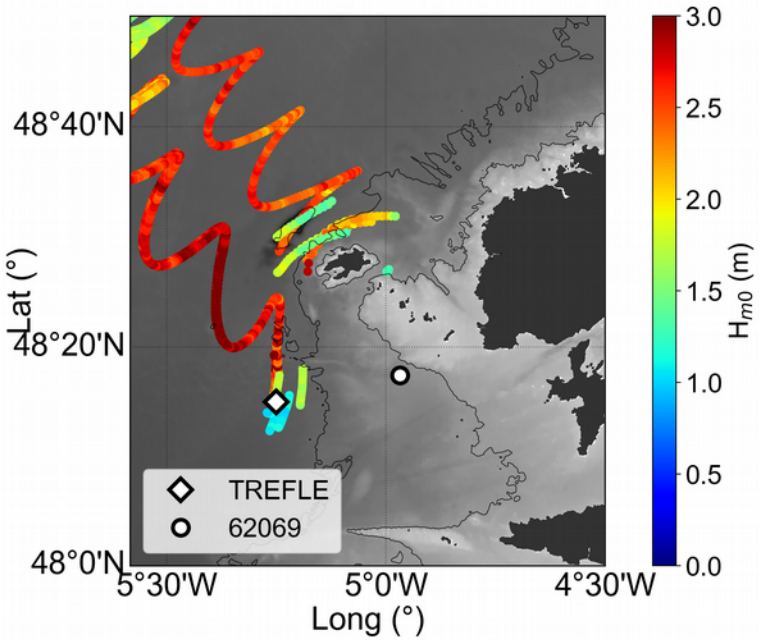

Figure 17: Map of the sea state observations collected during the campaign. The coloured lines mark the Spoondrift buoys trajectories, with colour corresponding to the significant waveheight H_{m0} measurements.

Figure 17 displays the significant waveheight observations collected during the campaign. Permanent moored instrumentation included the TREFLE buoy and the "Pierre Noire" buoy from the french national CANDHIS network, operated by CEREMA (WMO number 62069).

Spoondrift Spotter™ drifting buoys were deployed and recovered before and after KuROS / KaRADOC data collection flights, with the exception of SPOON01, SPOON06 and SPOON07. SPOON01 was deployed in the Keller Race area by the RIBs on 2018/11/21, escaped recovery, and drifted across the English Channel the subsequent days, while still transmitting its data. It grounded near the Needles lighthouse on the Isle of Wight on 2018/12/11, and could be recovered by ground. It thus provided a continuous timeseries of offshore sea state conditions during the whole campaign. SPOON06 and SPOON07 were deployed in the Offshore area by R/V Thalia on 2018/11/21 and escaped recovery until 2018/11/24, when the RIBs could take advantage of a very lenient day to dash and recover them. Figure 17 gives an overview of the large diversity of conditions encountered during the campaign, ranging from lenient (H_{m0} ~ 1 m) on 2018/11/24 and 2018/11/26, to well developed (H_{m0} ~ 3 m) on 2018/11/22. Also, the trajectories that cross the Keller Race area show a consistent pattern of spatial variability, significant waveheights being consistently larger in the western, more exposed, part of the area.

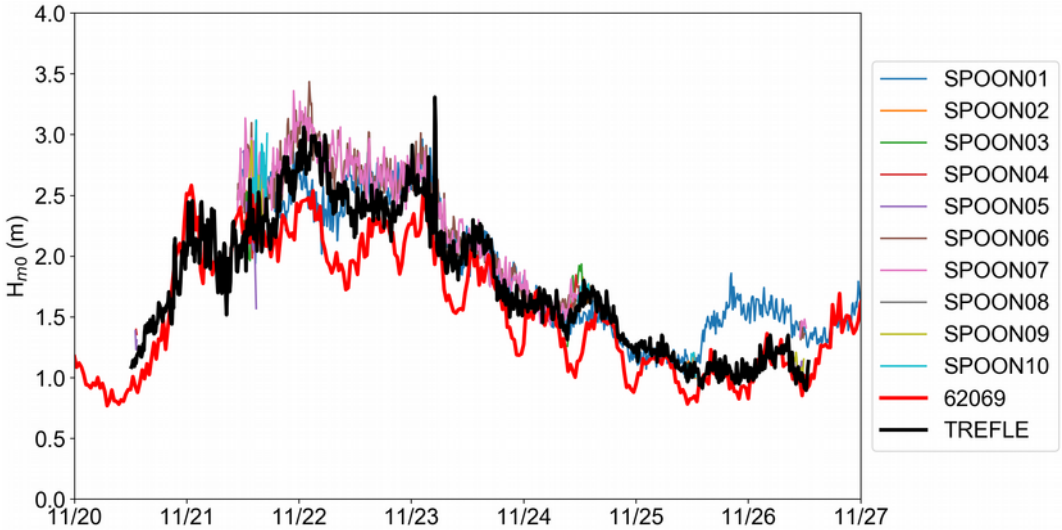

Figure 18: Significant waveheight H_{m0} timeseries collected by the different sea state measurement instruments deployed during the campaign.

Finally, Figure 18 shows the significant waveheight timeseries observed by the various platforms during the campaign. While all the different records show mainly similar evolutions, with a lenient sea state on 11/20, followed by a rapid increase to 3 m during 11/21, and a slow decrease back to 1 m on 11/26, interesting differences can be observed, which *a posteriori* highlight the importance of instrumenting the different observation areas: significant waveheight was for instance clearly lower at the rather sheltered position of buoy 62069 than at the TREFLE location. Significant waveheight was also strongly modulated by tidal currents at the location of buoy 62029, while the TREFLE buoy displayed little or no such modulation. Buoys SPOON06 and SPOON07 reported very consistent H_{m0} values during the night of 11/21 to 11/22, while they were drifting freely as a tighly packed pair, while buoy SPOON01, which was not very far, reported H_{m0} values smaller by roughly 0.5 m. The large discrepancy between SPOON01 and 62069 at the end of the record is due to the fact that SPOON01, which had not been recovered, was actually drifting more than 50 nautical miles to the north.

3 Conclusions and perspectives

Overall, the Drift4SKIM campaign can be considered extremely successful:

- It allowed the collection of a large set of airborne Doppler radar observations of the sea surface, both at Ku- and Ka-band, in two different acquisition geometries, relevant to several current or proposed satellite mission contexts, in a variety of conditions, together with a comprehensive set of ancillary measurements, documenting sea state and the structure of the sea surface, both from in-situ and optical remote sensing perspectives, eulerian and lagrangian currents over a large range of depths, and to some extent the meteorological conditions prevailing during the experiment. This dataset will be used for many years as a source of insight into the imaging mechanisms relevant to low-incidence Doppler microwave observations of the sea surface.
- A first analysis of the data, performed in the very tight timeframe of the preparation of the SKIM Report for Mission Selection [RD-6], has provided the basis for the validation of the Remote Sensing Spatial Simulator (R3S) [RD-7], a new electromagnetic simulation tool developed as part of the SKIM Phase A studies.
- This analysis required significant extensions of the theoretical framework used to describe Doppler radar observations of the sea surface. These development, collected in the Appendices of [RD-3], submitted as a research article to Ocean Science Discussions, pertain most notably to observation geometry, attitude correction requirements and requirements in terms of characterization of the instrument instantaneous Field Of View, and will be useful as guidelines in the design of future instruments, airborne as well as space-borne.
- This work has clearly highlighted the fact that direct transposition of airborne results to the spaceborne context is seldom, if at all, feasible, due to the very different acquisition geometries and instrument characteristics. Such a transposition requires an intermediate simulation stage, such as that provided by the R3S. A successful and lucid implementation of this simulation stage requires a thorough understanding of the imaging mechanism at play in the airborne acquisition used to validate the simulator, as well as of the adjustements necessary to carry out the extrapolation to the spaceborne context. The team involved in the Drift4SKIM 2018 experiment has greatly benefited from the opportunity, and has developed unique skills for these tasks.

However, due to he very tight timeframe in which this work has been performed, a number of interesting components of the dataset had to be left aside, which would be worth further investigation:

- though analysing airborne optical imagery to retrieve sea state information dates back to the 1954 paper by Cox and Munk, obtaining quantitative results remains very challenging. This could not be performed in the timeframe of the RfMS preparation, but the optical dataset is nevertheless of very high quality and should be analysed in this way, notably in conjunction with the in-situ sea state and Lagrangian surface drift datasets.
- little if any attention has been paid yet to the satellite radar acquisitions which were performed during the campaign, which include several S1A/B C-band SAR scenes,

several full polarization Radarsat 2 scenes, several Tandem-X scenes, and a S3A SRAL transect across the Offshore zone. These data should be studied in conjunction with the in-situ sea state measurements

- the ADCP and ADV mounted on the TREFLE buoy stopped providing useful data after the capsize of the structure in the morning of 11/22. This precluded their analysis in conjunction with the Doppler radar datasets, mainly collected on 11/22, 11/24 and 11/26, and they were thus left aside. These instruments provide however interesting observations of the Stokes and Eulerian surface shear in a rising wind context, which should be exploited. In the same spirit, though a cursory analysis of surface shear in the 0.4, 1, 2, 5, 15 m drogue depth buoy records has been performed, which concluded that in the quite energetic 11/22 conditions this shear was small enough to be neglected with respect to the Wave Doppler contribution, a more careful analysis of the dataset along this line should be conducted.

The Drift4SKIM campaign results, as presented in [RD-3], have however highlighted the very important role played by the estimation of the Wave Doppler contribution to the measured Doppler. In [RD-3] , this component was estimated based on in-situ sea state measurements. For lack of time, no attempts have been made to retrieve sea state characteristics based on KuROS or KaRADOC data.

In the broader perspective of the ongoing effort to ensure the launch and successful exploitation in the forthcoming years of a Doppler radar satellite devoted to the study of ocean TSCV, this is however a critical component of the signal processing chain, and it seems of utmost importance that a comprehensive assessment of the accuracy requirements on the sea state spectra estimation algorithm set by the need to estimate the Wave contribution to Doppler be carried out.

Present and planned elements on which to base this assessment include:

- Numerical simulations based on the R3S simulator. The capability of this simulator to reproduce Wave Doppler and backscattering signal statistics given sea state characteristics has been validated in [RD-3].

- Further analysis of the KuROS and KaRADOC datasets from the Drift4SKIM 2018 campaign. The KuROS radar in particular has been designed as a Cal/Val tool for the SWIM instrument onboard the CFOSAT satellite, which currently provides directional sea state estimates over the world ocean. The suitability of the algorithms developed for the analysis of KuROS data during the pre-launch phase to the estimation of Wave Doppler should be assessed. Improvements could be suggested, based on insight in the imaging mechanism obtained using the R3S simulations.

- Analysis of the SWIM data themselves. This instrument is functioning at Ku-band, and has no Doppler capability. Some elements of its acquisition geometry (incidence, scanning geometry) are however similar to the intended SKIM equivalents. Simulations of SWIM data using the R3S should thus allow to cross-check many elements of the transposition of airborne-data-based results to the spaceborne case.

- Analysis of KuROS and KaRADOC data to be collected during the airborne/in-situ data collection campaign SUMOS (Pis D. Hauser, P. Sutherland) planned for April 2020 in the Bay of Biscay. The airborne component of this campaign will involve both KuROS and an updated version of the KaRADOC instrument, while the in-situ component, performed from french R/V Thalassa, will involve an experimental array

in many ways similar to the Drift4SKIM one: three FLAMEs should be deployed, jointly with the TREFLE and a number of Spoondrift buoys, CARTHE and ODL drifters. During the majority of the flights, which will be devoted to SWIM calibration, the KuROS instrument will function in rotating mode, with KaRADOC performing continuous acquisitions in the port-looking cross-track direction. During a number of flights, funded by CNES as a contribution to the overall SKIM effort, star patterns will be performed over in-situ instrumentation, with both KuROS and KaRADOC functioning in the port-looking cross-track direction.

Acknowledgements

This study was supported by the KuROS4SKIM and DRIFT4SKIM contracts from the European Space Agency, made possible by the unflagging determination of Tania Casal, Craig Donlon and Erik de Witte.

The in situ measurements owe much to the dedication of the R/V Thalia crew.

Airborne data was obtained using the aircraft managed by Safire, the French facility for airborne research, an infrastructure of the French National Center for Scientific Research (CNRS), Météo-France and the French National Center for Space Studies (CNES). Many people at LOPS and OceanDataLab also contributed to the preparation, deployment and recovery of the instruments, including Ziad El Khoury Hanna, Gilles Guitton, Sylvain Herledan, Mickael Accensi, Pierre Branellec, Michel Hamon, Stéphane Leizour, Olivier Péden.

Many people at IETR are involved in the KaRADOC developments: Cécile Leconte, Mohamed Himdi, Paul leroy, Eric Pottier and especially Guy Grunfelder and Mor Diama Lo who have made possible the measurement campaign during November, 2018.

Operation of KuROS during the experiment would not have been possible without the dedication of Christophe Le Gac, Nicolas Pauwels and Christophe Dufour, from CNRS/LATMOS.